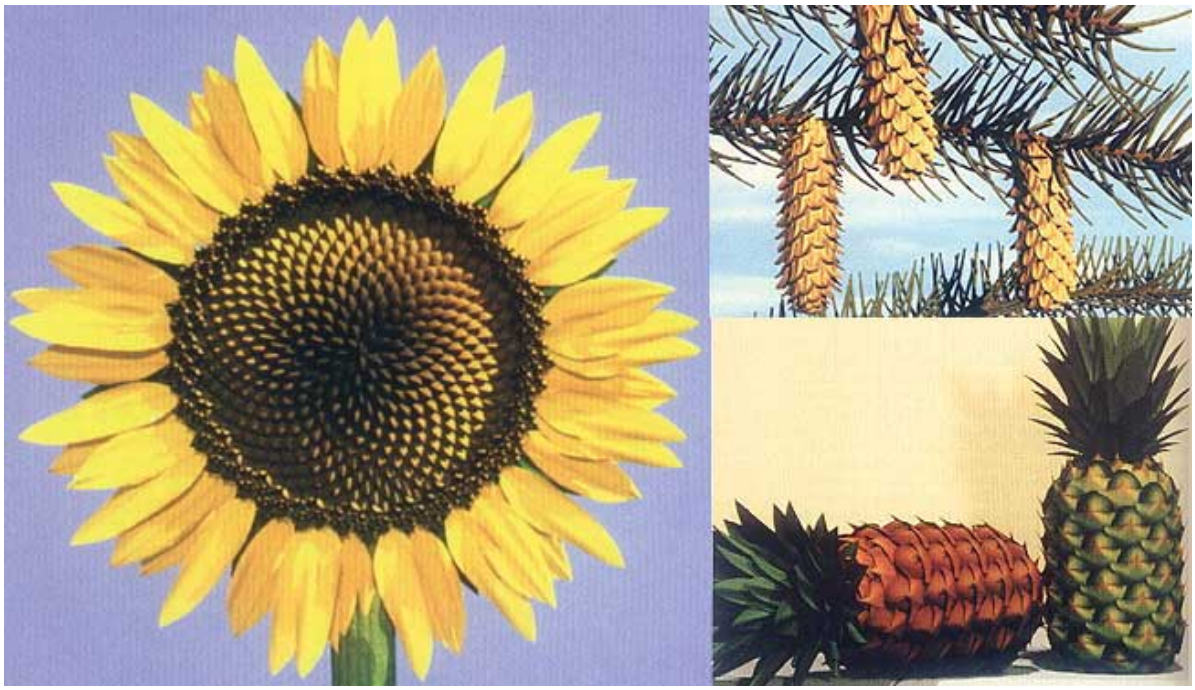

Recursive Sequences (1) The Fibonacci Sequence.

Let $u_n = \frac{1}{\sqrt{5}}\left[\left(\frac{1+\sqrt{5}}{2}\right)^n - \left(\frac{1-\sqrt{5}}{2}\right)^n\right]$, $n = 1, 2,$ ... show $u_1 = u_2 = 1$, $u_{n+1} = u_n + u_{n-1}$ by induction.

$u_1 = \frac{1}{\sqrt{5}}\left[\left(\frac{1+\sqrt{5}}{2}\right) - \left(\frac{1-\sqrt{5}}{2}\right)\right] = \frac{1}{\sqrt{5}}\left(\frac{2\sqrt{5}}{2}\right) = 1$, $u_2 = \frac{1}{\sqrt{5}}\left[\left(\frac{1+\sqrt{5}}{2}\right)^2 - \left(\frac{1-\sqrt{5}}{2}\right)^2\right] = \frac{1}{\sqrt{5}}\left(\frac{4\sqrt{5}}{4}\right) = 1,$

$u_{k+1} = u_k + u_{k-1} \Leftrightarrow \frac{1}{\sqrt{5}}\left[P^{k+1} - Q^{k+1}\right] = \frac{1}{\sqrt{5}}\left[P^k - Q^k\right] + \frac{1}{\sqrt{5}}\left[P^{k-1} - Q^{k-1}\right]$

$\Leftrightarrow P^{k-1}(P^2 - P - 1) + Q^{k-1}(Q^2 - Q - 1) = 0$, but both P and Q are solutions of $x^2 - x - 1 = 0$ so true.

We thus find $\{u_n\} = 1, 1, 2, 3, 5, 8, 13, 21, 34, 55, 89,$ ... has the values of the Fibonacci sequence.

The ratio of successive terms $\frac{u_{n+1}}{u_n} = \frac{u_n}{u_n} + \frac{u_{n-1}}{u_n}$ tends to $r = 1 + \frac{1}{r}$, which again is solved by P and Q.

In fact $P/1 = 1/(-Q) = r$, as can be seen from the fact that the product of the roots is 1 in $x^2 - x - 1 = 0$.
This is the fabled Golden Mean which is the ratio preserving the dimensions of the classic rectangle when a square is removed.. Note: $-Q > 0$.

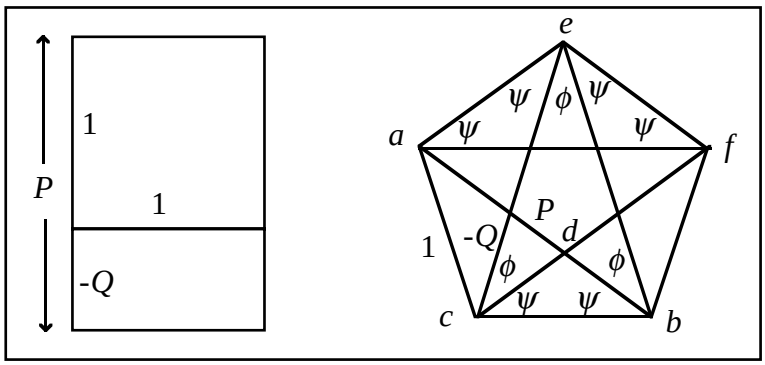

This also occurs in the pentagram. From Δebc $3\phi + 2\psi = \pi$, Δeaf $\phi + 4\psi = \pi$, giving $\phi = \psi = \frac{\pi}{5}$.

Now Δabc Δdbc are similar, giving $P/1 = 1/(-Q)$. Hence $\cos(\pi/5) = P/2$, $\cos(2\pi/5) = -Q/2$, etc.

The Fibonacci sequence also plays a pivotal role in nature. The Fibonacci angle $\theta_f = \frac{2\pi}{P^2} \approx 137.5^\circ$ is pivotal in plant form appearing in the sunflower, cacti pineapple, pine cones and other plant growth forms in which two interlaced spirals return values of Fibonacci numbers, e.g. 34 and 55 in the case of the sunflower above and the 8 and 13 spirals of the pineapple as Coxeter noted each generated by a mathematical L-system from "The Algorithmic Beauty of Plants" by Prusinkiewicz and .Lindenmayer.

The derivation of this relatonship between angle and series is complex and not fully researched, but it is based on the idea of a constant angle of rotation which minimizes the overlap between successive florets caused by "mode locking" periodicities and is very sensitive to small changes as noted below.

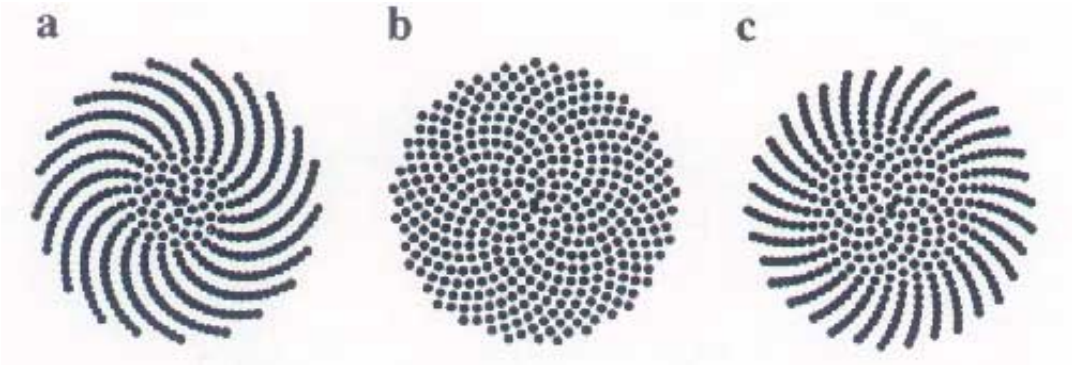

Figure 4.2: Generating phyllotactic patterns on a disk. These three patterns differ only by the value of the divergence angle α, equal to (a) 137.3°, (b) 137.5° (the correct value), and (c) 137.6°.

Recursive Sequences (2) The Logistic Iteration.

To appreciate the complex diversity in recursive iterated functions, we will examine a typical quadratic iteration, the logistic map :

$$x_{n+1} = G_r(x_n) = r\, x_n\, (1 - x_n)$$

representing exponential population growth subject to a constrained area. This is an issue central to the future survival of human population explosion from boom and bust and also to natural populations. The term $r.x_n$ provides exponential growth while the additional term $(1 - x_n)$ places a finite remaining area, for food resuorces to sustain the increase, constraining the population.

It is easy to picture such an iteration in various ways. One is to successively evaluate the functions $y = r\, x\, (1 - x)$ and $x = y$ as shown in fig 4(b_i). We pick an initial value x and evaluate y by moving vertically to the parabola. Next we let x = y by moving horizontally to the sloping line. The two steps combined result in one iteration i.e. $x_{n+1} = y = r\, x_n\, (1 - x_n)$.

As the parameter r varies, the behavior of the iteration goes through a sequence of different stages. In (b_i) the iterations are illustrated for r = 1 and 2 starting from two arbitrary points in [0,1]. Each iterates toward a fixed point, one at zero and the other positive. For the remaining figures the iteration is left to run for a few hundred steps, before plotting, so that only the limiting attractor is highlighted. Near the value 3.4 the iteration is attracted to an alternating set of two values, i.e. period 2, as depicted in (b_{ii}), in which the arrows still indicate the $y = r\, x\, (1 - x)$ and $x = y$ steps. At 3.56, (b_{iii}), the period 2 orbit has bifurcated twice to form a period 8 orbit. The effect of such period doubling is is clearly seen in the braided form of the attractor path. At 3.66, (b_{iv}), chaos has set in and the orbits now spread irregularly across the interval without returning exactly. At 3.8282 (b_v) we are very close to the period 3 window. The period 3 iteration keeps slipping however, and intermittently enters chaos before returning to the attractor. At 3.8289 (b_{vi}) period 3 has become stable. At 4.5 (c) the attractor has broken up and now most points escape to $-\infty$. A residual Cantor set of points (the Julia set) is mapped chaotically amongst itself.

Alternatively, we can plot all the x values that occur for a given r, once the system has been allowed to approach the attractor, as shown in fig 4(a). This gives rise to the *attractor form* diagram in which an initial point attractor repeatedly bifurcates into 2, 4, 8, ... values limiting in chaos at r_∞, punctuated by further

windows e.g. of period 3, and finally breakup of the attractor at r = 4.

Corresponding values of the *Liapunov exponent* representing the degree of exponential spreading are shown below this. For $r < r_\infty$, $\lambda \leq 0$, reaching zero at each bifurcation point r_i , but once chaos begins, $\lambda > 0$, except for brief negative dips in the periodic windows.

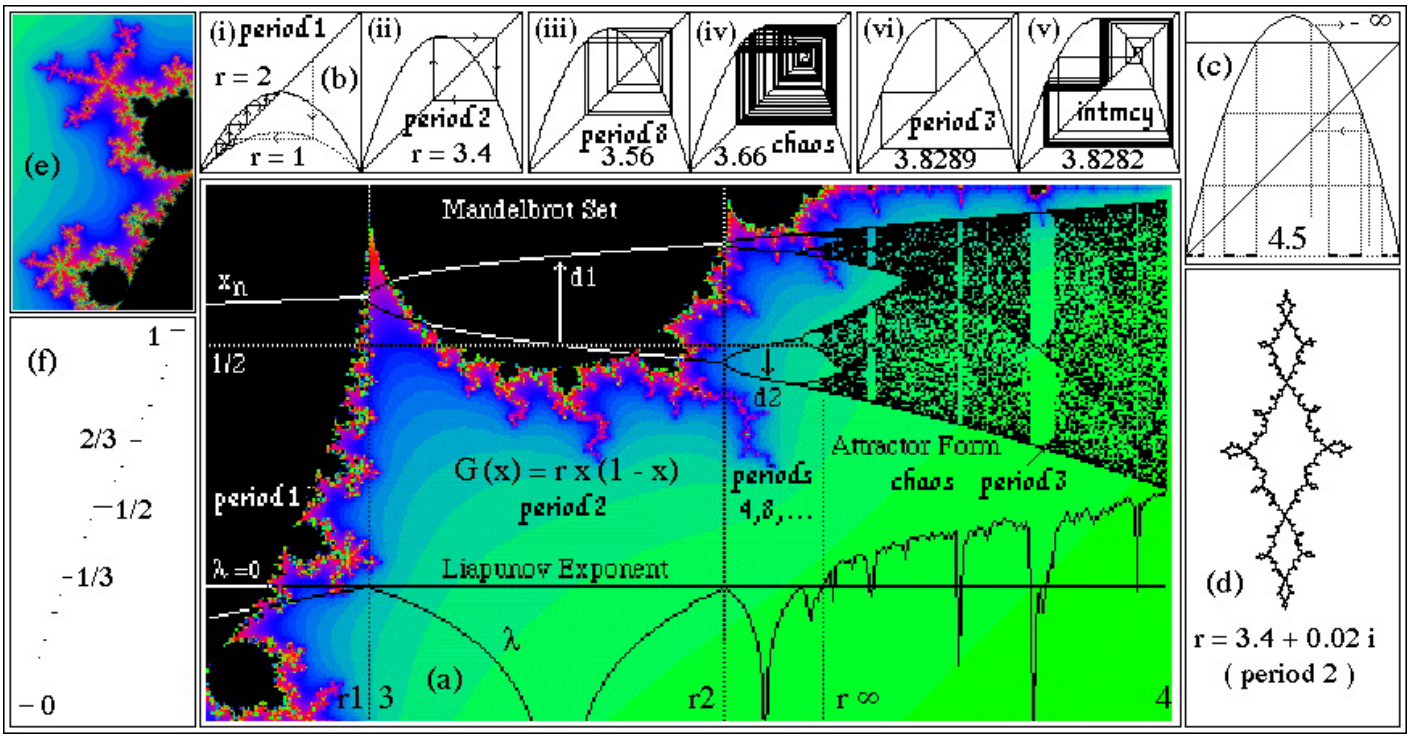

The Logistic iteration (a) The attracting limit sets, Liapunov exponent and Mandelbrot set, for $2.8 \leq r \leq 4$ showing multiple period doublings, chaotic regions and periodic windows. The limit attractor initially is a single curve (point) but then repeatedly subdivides in period doublings to period 2, 4,8, etc. finally entering chaos (stippled band). Subsequently there are windows of period 3, 5 etc. with abrupt transitions from and to chaos caused by intermittency and crises. The Liapunov exponent λ measauring exponential spreading (chaotic sensitive dependence) negative or zero until chaos sets in. During chaos it remains positive. The Mandelbrot set illustrates the fractal nature of the periodic and chaotic regimes when x & r are extended to the complex number plane. All points in side thi set have r values leading to finite periodic attractors. Complex number representation aids visualizing fractal processes. (b) A series of 2-D iterations of $G_r(x_n)$ including periods 1, 2 and 8 chaos, intermittency, and period 3. In (i) the two-step iteration process is illustrated alternately evaluating y = r x (1 - x) (vertical) and x = y (horizontal). As r crosses the value 1 a saddle-node bifurcation occurs resulting in the attractor moving from zero and leaving a repellor there (r = 2). In (ii) & (iii) period 2 and 8 attractors have formed. In (iv) the iteration has become chaotic. In (v) the chaos is intermittently entering a period 3 regime, which has become stable in (vi). (c) Mode-locking trransition is illustrated in the preiodicities of the bulbs on the Mandelbrot set, the right hand bulb's dendrites indicating a periodicity of five per revolution. (d) The fractal julia set of chatic values for one particular complex value of r. (e) The Cantor set for real r >4, (f) the devils staircase of mode-locking intervals.

Diverse Dynamics in the Logistic map :

(1) **Point attractors :** When r = 0 the attractor is initially zero. As the parameter r is increased from 0, the quadratic rises and at 1 crosses the line y = x resulting in a **saddle-node** bifurcation in which a single attractor becomes a pair : an attractor and a repellor. In higher dimensional situations we would have a saddle, fig 6(c) and an attractor or repellor (node). The point attractor moves up to positive x, leaving a repellor at 0. Outside [0,1] the iteration tends to - ∞. This situation is illustrated in fig 4(bi) where for the transitional value r = 1 the iteration is still attracted down and to the left to zero, while for r = 2, zero is a *repellor* and the intersection of the parabola with the line y = x is an *attractor*.

(2) **Period doubling :** At value $r_1 \sim 3$ there is a bifurcation of the fixed attractor into a period 2 attracting set, as illustrated in (bii). Successive period doublings at r_2 etc., (bii, iii) cause the attractor to have a sequence of periods 2, 4, 8, ... , 2^n. These arise from **pitchfork bifurcations** as illustrated obviously in the forkings of attractor form in (a). Here the graph of the two-step iterate $G_r^2(x) = G_r(G_r(x))$ twists across y = x to cause a

doubling of the period. In this range the Liapunov exponent $\lambda < 0$, except at r_1, r_2, etc. where $\lambda = 0$. In (a) are outlined the bifurcation values r1, r2, ..., r∞ and the distances d1, d2, ... where d_n are the widths of the period 2^n attractors where they straddle the symmetrical value 1/2.

The values $r_n = r_\infty - Cd^{-n}$ and $d_n = \frac{d_{n-1}}{-\alpha}$ are determined by the **Feigenbaum numbers** d = 4.669, and a = 2.502. These are universal to all functions with a polynomial type maximum and thus appear in a variety of systems from biology to astronomy (Stewart 1989).

(3) **Chaos :** At the limit value r_∞ the iteration becomes chaotic, (biv) and l > 0. The trajectories now spread over the interval [0,1]. They do not recur as there are no finite periodicities, but approach each possible value arbitrarily closely given sufficient time. The iteration now has sensitive dependence, e-close initial points becoming exponentially separated. Although the orbits appear equally spread across the entire possible range of values, the details of each are structurally unique. Complexity grammars (Auerbach & Procaccia (1990) further analysis.

(4) **Odd Period Windows : Intermittency and Crises** There are a series of windows in the chaotic region where chaotic behavior is abruptly interrupted by new periodic regimes of periods 3, 5, etc., (bvi). These windows contain for example 3.2^n bifurcation sequences similar to that of (2). The existence of a period 3 attractor guarantees the existence of periods of all orders and uncountably many aperiodic orbits (chaos). By Sarkovski, the periods follow the causal sequence :

$$3 \rightarrow 5 \rightarrow 7 \ldots 2^n.3 \rightarrow 2^n.5 \rightarrow \ldots 2^4 \rightarrow 2^3 \rightarrow 2^2 \rightarrow 2 \rightarrow 1 \qquad n = 1, 2, 3,\ldots$$

At the left-hand end of the period 3 window, a new type of bifurcation, the **tangent bifurcation** occurs, in which the 3-cycle becomes intermittently disrupted by chaotic bursts, (bv). Intermittent disruption of a periodic dynamic constitutes a second route to chaos distinct from period doubling in which only a single bifurcation is required for chaos. At the right-hand end of the period 3 window is another type of abrupt transition to chaos called a **crisis** that is caused by a collision between a point repellor and the fanning chaotic sub-bands of period 3 forming small triangles in fig 4(a). This causes the chaos to be repelled so that it spreads suddenly across all values again. The 3 repellors originate from the birth of period 3 in the tangent bifurcation at the other end of the window.

(5) **Julia sets and Horseshoes :** For each value of r there is a residual fractal Julia set of exceptional points which do not converge to the attractors, but are mapped instead among themselves. The Julia set for an r value of the complex logistic map in the period 2 region is illustrated (d). Complex values assist the visualization of Julia sets because complex numbers form a planar image which we can see.

For r > 4 the finite attractor ceases to exist, since the graph now goes outside the unit square, allowing points to iterate to - ∞, however a Cantor set of points remains, fig 4(c) which are mapped among themselves indefinitely, once all the points which escape to -∞ in one or more stages are removed. This is the Julia set of the mapping, which in this case is not a connected set, because of the destruction of the finite attractor's basin.

(6) **Mode locking :** As r varies around the boundary of the Mandelbrot set (c) above the neutral dynamic becomes mode locked into rational frequency relationships. Between these there is an irrational flow. This phenomenon relates closely to the non mode-locked sunflower at the Fibonacci angle. The mode-locked values form a Devil's staircase (f) of ordered rational values as shown in (f), in which successive rational periodicities each have an interval over which resonance occurs.